IEEE Access
Multidisciplinary : Rapid Review : Open Access Journal

Received 28 June 2022, accepted 19 July 2022, date of publication 4 August 2022, date of current version 12 August 2022.
Digital Object Identifier 10.1109/ACCESS.2022.3196357

RESEARCH ARTICLE

An Alternative Methodology for Quantifying Voltage Unbalance Based on the Effects of the Temperatures and Efficiency of Induction Motors

MARCOS D. C. SILVA AND ANÉSIO DE L. FERREIRA FILHO
Engineering Department, Universidade de Brasília, Brasília, Distrito Federal 70910-900, Brazil
Corresponding authors: Marcos D. C. Silva (mdiego86@gmail.com) and Anésio de L. Ferreira Filho (leles@ene.unb.br)

ABSTRACT Many unbalanced voltage conditions, which produce different effects on electric equipment, are associated with the same voltage unbalance factor. This fact hinders the precise association between the values of this index and the effects of voltage unbalance. In the present study, an alternative methodology for quantifying voltage unbalance based on the effects of this phenomenon on the temperature and efficiency of three-phase induction motors is proposed. The application of the suggested methodology results in an index that contemplates the combined effects of the modules and angles of the positive and negative sequence voltages. Aiming to apply this methodology and evaluate its performance, we selected a comprehensive set of balanced and unbalanced voltage conditions and used it on a three-phase induction motor. The results show that the index obtained, when compared to the traditional voltage unbalance factors, reduces the uncertainties inherent to the quantification process of this phenomenon. In other words, it allows a better association between the values and effects of the voltage unbalance. For these reasons, this index is considered as a potential alternative that can be employed in industrial utilities and standards that deal with voltage unbalance.

INDEX TERMS Efficiency, index to quantify voltage unbalance, induction motor, power quality, symmetrical components, temperature.

I. INTRODUCTION

Voltage unbalance (VU) is a power quality phenomenon that occurs in electric systems when there is any inequality between the modules of three-phase voltages and/or angular lags different from 120°. If not properly quantified, it can economically affect industrial consumers by reducing the efficiency (η) and lifetime of equipment and can lead to incorrect decision-makings regarding the motor derating and protective system, for instance.

In the literature, it is possible to find works whose approaches essentially contemplate the effects of this phenomenon on devices of the power system [1]–[3], and also those in which these effects are used to verify the limitations of the indexes employed in its quantification [4]–[7].

In [1], the analysis of the oscillations caused by unbalanced loads in salient pole synchronous generators was highlighted, in order to identify and quantify the magnitude of the electromagnetic torque caused by unbalanced currents. In [2], it was presented a comparison of the harmonic response of three different efficiency classes of three-phase induction motors (TIM) in the presence of voltage harmonics and unbalance with voltage variations. In [3], an investigation of the influence of unbalanced and nonsinusoidal voltages on power factor definitions and measurement algorithms was made considering a constant impedance load and a TIM.

Some authors [4]–[8] have investigated the limitations of the indexes employed to quantify the VU. They mentioned, among several other aspects, that many unbalance conditions,

The associate editor coordinating the review of this manuscript and approving it for publication was Nagesh Prabhu.

which produce different effects on electric equipment, are associated with the same index used to quantify VU. This type of limitation can be observed when employing either the voltage unbalance factor (VUF), the index calculated using the symmetric components, the line voltage unbalance rate (LVUR) proposed by the National Electrical Manufacturer's Association (NEMA), or the phase voltage unbalance rate (PVUR) presented by the IEEE. For this reason, research has emphasized the incapacity of these indexes to properly correlate the levels of unbalance with their effects and, in some of these works, proposals of procedures for quantifying VU were presented.

In [4], the VU was categorized into eight types, according to the magnitudes (under and over-voltage) and the phase angles of the three-phase voltages derived from the VU. The authors concluded that the different groups of VU have different effects on a TIM. To mitigate this problem, the use of the module of positive sequence voltage component (V_1) together with the VUF was suggested. In [5], an electrical model of a TIM was used to evaluate the performance of the electric machine, running at steady state, submitted to several conditions of the complex voltage unbalance factor (CVUF) and with the V_1 equal to the rated voltage. It was found that for a constant level of VUF, the maximum stator currents, the maximum allowable slip, and the derating factor may vary according to the values of the VUF and the angular difference (θ_2) between the phasors $\overline{V}_1$ and $\overline{V}_2$ (respectively, the voltage components of the positive and negative sequences). Therefore, both VUF and θ_2 (i.e., the CVUF) must be considered to provide a global picture of the effects of the VU on the motor operation. In [6], it was demonstrated that the joint use of CVUF amplitude and angle with V_1 makes it possible to associate the values of these quantities with an effect, i.e., a single TIM power or efficiency value. In other words, when using the CVUF, assigning a constant value to V_1 leads to a specific VU case. In [7], the authors employed the complex current unbalance factor (CCUF) to determine the output power of industrial induction motors subjected to VU. In this study, the CCUF was calculated by means of an electric model whose parameters depend on the characteristics of the machine under evaluation. Given it is an index based on the analysis of current, the results of its application are restricted to the loads responsible for generating the positive and negative sequence currents used in its calculation. In [8], the dependency of the TIM derating aspects on CVUF was investigated. In this study, tests were carried out under various VU conditions to examine the effect of the VUF, the V_1, and the CCUF angle. The outcomes revealed that the motor derating is dependent on the complex nature of VU. Thus, the angle of CVUF or CCUF and the V_1 should also be considered when determining the effective derating levels of a TIM.

From the mentioned works, it is possible to note that the joint use of V_1 with the VUF and of θ_2 with the VUF has been suggested and employed by some specialists for the VU quantification process. However, these procedures have not been proven to be effective as a method to quantify unbalance. The main reason for this is that when more than one variable is utilized simultaneously, the process of establishing the compatibility levels of these quantities becomes more complex. In fact, there is a lack of studies that address the joint effects of the variables responsible for the VU in a single index. Moreover, it should be noted that there are no recent studies in the literature that suggest an index whose proposition has been elaborated based on the relation between its magnitude and the effects of VU, identified through experimental tests.

In this work, an alternative methodology for the quantification of VU based on the effects of this phenomenon on the temperature and η of TIM is presented. The application of this methodology culminates in an index that reduces the uncertainties inherent to the quantification procedures of VU. To apply this methodology and evaluate the performance of the index obtained, we selected a comprehensive set of balanced and unbalanced voltage conditions and used it on a TIM.

According to [6], TIM is widely utilized in industrial, residential and commercial systems. While [9]–[13] affirm that in a typical industry, the TIM constitutes about 70% to 80% of the loads. In the literature, studies related to the VU [1]–[10] investigate heating, reduction in the η, torque, vibrations, request of insulation, derating factor, or TIM lifetime loss. Considering these aspects, we opted to use the temperatures and η acquired from a TIM in the proposed methodology.

As the main contribution of this study, we can mention the fact that a new methodology is proposed whose application allows obtaining a new index for the VU quantification. Such index has a promising application potential, allowing the unbalance to be measured in a more accurate way, since it correlates its magnitude with the effects of VU on the temperatures and η of a TIM.

In the section that follows, some concepts and the alternative methodology are presented. We then describe the databases with balanced and unbalanced voltages and the laboratory apparatus employed in this work to acquire the temperature and η of the TIM tested. Subsequently, the results from the application of the methodology and the evaluation of the obtained index are shown. Finally, we present our concluding remarks.

II. QUANTIFICATION OF VOLTAGE UNBALANCE

In the literature and in normative documents, different VU calculation methodologies can be found. Some standards and recommendations, such as the IEEE 1159-2009 [14], IEC 61000-4-30 [15], NRS 048-2 [16], and the Brazilian Distribution Procedures – PRODIST [17], that deal with VU quantification, employ VUF index defined as:

$$\mathrm{VUF}\,(\%) = V_2 / V_1 \times 100 \tag{1}$$

where V_2 is the module of $\overline{V}_2$.

In [18], [19], the VUF is considered the true unbalance index. According to IEEE std. 1159, this method is the most reliable, as it directly represents the phenomenon of VU without approximations.

Another index used to quantify VU is LVUR, which is given by (2), according to the NEMA definition [20].

$$\text{LVUR}\,(\%) = \Delta V_{\text{Line,Max}} / \Delta V_{\text{Line,Mean}} \times 100 \tag{2}$$

where $\Delta V_{\text{Line,Mean}}$ is the arithmetic mean of the line voltages and $\Delta V_{\text{Line,Max}}$ is the maximum deviation between the measured line voltages and $\Delta V_{\text{Line,Mean}}$.

The index PVUR, presented by IEEE Std. 141-1993 [18] and [21], is calculated according to (3).

$$\text{PVUR}\,(\%) = \Delta V_{\text{Phase,Max}} / \Delta V_{\text{Phase,Mean}} \times 100 \tag{3}$$

where $\Delta V_{\text{Phase,Mean}}$ is the arithmetic mean of the phase voltages and $\Delta V_{\text{Phase,Max}}$ is the maximum deviation between the measured phase voltages and $\Delta V_{\text{Phase,Mean}}$.

III. A NEW METHODOLOGY TO QUANTIFY VOLTAGE UNBALANCE

With the formulation of the VUF, LVUR and PVUR in (1) to (3), it is verified that the influence of i) the angle θ_2, ii) the nominal voltage (V_{NOM}), and iii) the non-linear characteristics of the temperature and η of electric equipment in relation to the variations of $\overline{V}_2$ and $\overline{V}_1$ are not considered in the conceptualization of the traditional indexes employed to quantify the VU.

Moreover, as previously highlighted, several unbalanced voltage conditions result in the same VUF, LVUR and PVUR. Such limitations hinder the precise association between the values of these indexes with the effects of VU. These aspects led to the idea of developing an alternative methodology for quantifying VU based on the effects of the temperatures and η of TIM.

Considering the above-mentioned aspects, we proposed a methodology, whose application resulted in an index to quantify the VU, referred to as the weighted voltage unbalance factor (WVUF). This methodology consists of the steps described in the following subsections.

A. APPLICATION OF THE BALANCED AND UNBALANCED VOLTAGE CONDITIONS TO THE TIM

The first stage of this methodology is intended to obtain the temperatures and η of TIM. For this, we applied several balanced and unbalanced voltage conditions (that comprise a database) to the TIM and recorded the readings of η and the critical temperature (T), which correspond to the highest temperature between the three phases of the stator windings. The data banks of balanced and unbalanced voltage conditions and the laboratorial apparatus employed to collect the temperatures and η of the TIM under test are described in the next section.

B. MODELING THE AVERAGE BEHAVIOR OF THE TIM TEMPERATURE AND EFFICIENCY VARIATIONS

In the second stage, the objective is to model the average behavior of the variations of the T and η of TIM in relation to V_2, V_1 and θ_2. To obtain these models, it is needed to identify all sets of curves of the T and η of the TIM in function of V_2, V_1 and θ_2, by applying numerical regressions. By doing this, we will obtain three sets of T curves as a function of V_2, V_1 and θ_2, which are defined according to (4) to (6), and the other three sets of η curves as a function of V_2, V_1 and θ_2, which are defined in accordance with (7) to (9).

$$ST_{V2} = \left\{ST^1_{V2}(V_2); ST^2_{V2}(V_2); \ldots; ST^N_{V2}(V_2)\right\} \tag{4}$$

$$ST_{V1} = \left\{ST^1_{V1}(V_2); ST^2_{V1}(V_2); \ldots; ST^N_{V1}(V_2)\right\} \tag{5}$$

$$ST_{\theta 2} = \left\{ST^1_{\theta 2}(\theta_2, V_2); ST^2_{\theta 2}(\theta_2, V_2); \ldots; ST^N_{\theta 2}(\theta_2, V_2)\right\} \tag{6}$$

$$S\eta_{V2} = \left\{S\eta^1_{V2}(V_2); S\eta^2_{V2}(V_2); \ldots; S\eta^N_{V2}(V_2)\right\} \tag{7}$$

$$S\eta_{V1} = \left\{S\eta^1_{V1}(V_2); S\eta^2_{V1}(V_2); \ldots; S\eta^N_{V1}(V_2)\right\} \tag{8}$$

$$S\eta_{\theta 2} = \left\{S\eta^1_{\theta 2}(\theta_2, V_2); S\eta^2_{\theta 2}(\theta_2, V_2); \ldots; S\eta^N_{\theta 2}(\theta_2, V_2)\right\} \tag{9}$$

After that, the average curves for each of the six sets of (4) to (9) must be calculated. These six average curves are defined respectively as $AT_{V2}(V_2)$, $AT_{V1}(V_1)$, $AT_{\theta 2}(\theta_2,V_2)$, $A\eta_{V2}(V_2)$, $A\eta_{V1}(V_1)$ and $A\eta_{\theta 2}(\theta_2,V_2)$.

The last part of this step consists in the elimination of the constant values (offsets) of the average curves and the inversion of the three curves of η, which are decreasing. The six curves resulting from this procedure are defined respectively as $BT_{V2}(V_2)$, $BT_{V1}(V_1)$, $BT_{\theta 2}(\theta_2,V_2)$, $B\eta_{V2}(V_2)$, $B\eta_{V1}(V_1)$ and $B\eta_{\theta 2}(\theta_2,V_2)$.

C. MODELING THE JOINT WEIGHTED AVERAGE BEHAVIOR OF THE TIM TEMPERATURE AND EFFICIENCY VARIATIONS

In the third stage, we aimed to model the weighted average behavior resulting from the joint approach of the variations of the T and η of TIM in relation to V_2, V_1 and θ_2. These behaviors are represented by the models named $F(V_2)$, $G(V_1)$ and $H(\theta_2,V_2)$. The $F(V_2)$ represents the weighted average behavior resulting from the joint approach of the variations of the T and η of TIM in function of V_2, and $G(V_1)$ and $H(\theta_2,V_2)$ are related to V_1 and θ_2, respectively. With the intention of obtaining the $F(V_2)$, $G(V_1)$ and $H(\theta_2,V_2)$ and to make it possible to associate the T and η in a joint average model, changes are initially performed in the scales of these quantities. Next, the selection of the weights that represent the contribution of T and η on the mentioned models are applied.

It is important to emphasize that $BT_{V2}(V_2)$, $BT_{V1}(V_1)$ and $BT_{\theta 2}(\theta_2,V_2)$ have a scale of magnitude (temperature in degree Celsius), and $B\eta_{V2}(V_2)$, $B\eta_{V1}(V_1)$ and $B\eta_{\theta 2}(\theta_2,V_2)$ have another scale (efficiency in percentage). For this reason, normalizations are applied so that the proportions between the curves of T and η are maintained. Therefore, $BT_{V2}(V_2)$, $BT_{V1}(V_1)$ and $BT_{\theta 2}(\theta_2,V_2)$ are multiplied by a normalization factor 'α' and $B\eta_{V2}(V_2)$, $B\eta_{V1}(V_1)$ and $B\eta_{\theta 2}(\theta_2,V_2)$ are multiplied by a factor 'β'. This way, we obtain a set of curves defined as $CT_{V2}(V_2)$, $CT_{V1}(V_1)$, $CT_{\theta 2}(\theta_2,V_2)$, $C\eta_{V2}(V_2)$, $C\eta_{V1}(V_1)$ and $C\eta_{\theta 2}(\theta_2,V_2)$.

D. FORMULATION OF THE WVUF

The index WVUF is formulated as shown in (10).

$$WVUF(\%) = F(V_2) + G(V_1) + H(\theta_2, V_2) \quad (10)$$

where:

$$F(V_2) = W_F \cdot CT_{V2}(V_2) + (1 - W_F) \cdot C\eta_{V2}(V_2) \quad (11)$$

$$G(V_1) = W_G \cdot CT_{V1}(V_1) + (1 - W_G) \cdot C\eta_{V1}(V_1) \quad (12)$$

$$H(\theta_2, V_2) = W_H \cdot CT_{\theta 2}(\theta_2, V_2) + (1 - W_H) \cdot C\eta_{\theta 2}(\theta_2, V_2) \quad (13)$$

W_F, W_G and W_H are the values of the weights (in the range between 0 and 1) assigned to the T in the $F(V_2)$, $G(V_1)$ and $H(\theta_2,V_2)$ functions, that compose the WVUF.

From (11) to (13), we can observe that different combinations of weights W_F, W_G and W_H can be chosen for the formulation of the WVUF. In summary, if $W_F = W_G = W_H = 1$, the WVUF will only include the effects of the T in its formulation. Complementarily, if $W_F = W_G = W_H = 0$, only the effect of the η will be considered. And lastly, if $W_F = W_G = W_H = 0.5$, this means that the same weights are assigned to both T and η.

The WVUF formulated according to (10) is capable to correlate the effects of the variations of the T and η of TIM with V_2, V_1 and θ_2. Thus, the different contributions of the modules and angles of $\overline{V}_2$ and $\overline{V}_1$ are contemplated.

It should be highlighted that the proposed methodology can be applied to a set of temperatures and η acquired from TIM with different power ratings and load conditions. In the case of using many TIM, there is the need to get the average behavior of the variations of the T and η considering all of them simultaneously. Once the WVUF is obtained, it can be employed to quantify the VU without the need of repeating the steps highlighted above. Since it is a methodology based on the use of real data of the temperature and η of TIM, the results of its application presented in Section V provide details of each one of the steps that constitute it.

In this work, we disregarded the effects of the zero-sequence voltage component ($\overline{V}_0$), since three-phase electrical devices are usually connected without path to neutral. However, there are pieces of equipment, such as power transformers (inherently intrinsic to transmission and distribution systems), which are regularly connected to four wires. Furthermore, it is known that the circulation of zero-sequence currents contributes to the formation of VU, which can occur due to the presence of two-wire electrical loads unevenly distributed between the phase voltages, or also due to ground-related faults, for example.

Although the influence of $\overline{V}_0$ was not considered in the analysis that follows, it is important to make it clear that the proposed methodology could be extended to include the effects of this component. Conceptually, the idea for applying the methodology with the results from four-wire loads is the same. In this scenario, the effects of $\overline{V}_0$ (module and angle) should be considered in the formulation of the index used to quantify the VU.

In the next section, the data banks with the terminal voltages used to obtain the T and η of the utilized TIM and the laboratory infrastructure are displayed. Furthermore, the thermal model of the TIM employed to estimate the temperatures in steady state operation is detailed.

TABLE 1. Composition of the data bank DB_1.

Specification	Values
V_1	200 V to 232 V in steps of 4 V
V_2 (% of V_{NOM})	0%; 0.5%; 1.0%; ... ; 7.5%
θ_2	0° to 360° in steps of 6°

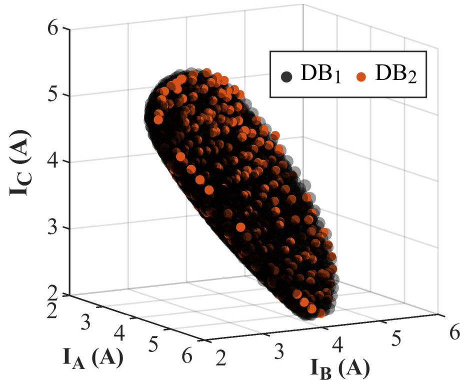

FIGURE 1. Phase currents of the TIM read from the application of databases DB_1 and DB_2.

IV. EXPERIMENTAL SETUP

A. THE DATA BANKS WITH THE BALANCED AND UNBALANCED VOLTAGES

In the analysis performed in this study, the three-phase electric currents (I_A, I_B and I_C) and η of the TIM under test were obtained via real laboratory measurements. The temperatures were obtained indirectly, using the I_A, I_B and I_C as the input of a thermal model. For this, we elaborated the data bank named DB_1 with a set of 8244 balanced and unbalanced three-phase voltages to cover several VU conditions. Each DB_1 condition is applied to the TIM under test for 30 seconds, time which is enough for reading the electric currents and the input and output powers at steady state. However, some temperature measurements are also performed to identify the parameters of the thermal model and to validate it. Therefore, we elaborated the data bank DB_2, in which each VU condition remains imposed on the TIM for 16 minutes. This time is required for reading the steady state temperature.

Table 1 shows the values of V_1, V_2 and θ_2 that constitute the conditions of DB_1. From this, it is possible to observe that the variation adopted for V_1 in DB_1 contemplates the range of voltages established as adequate (from 92% to 105% of the

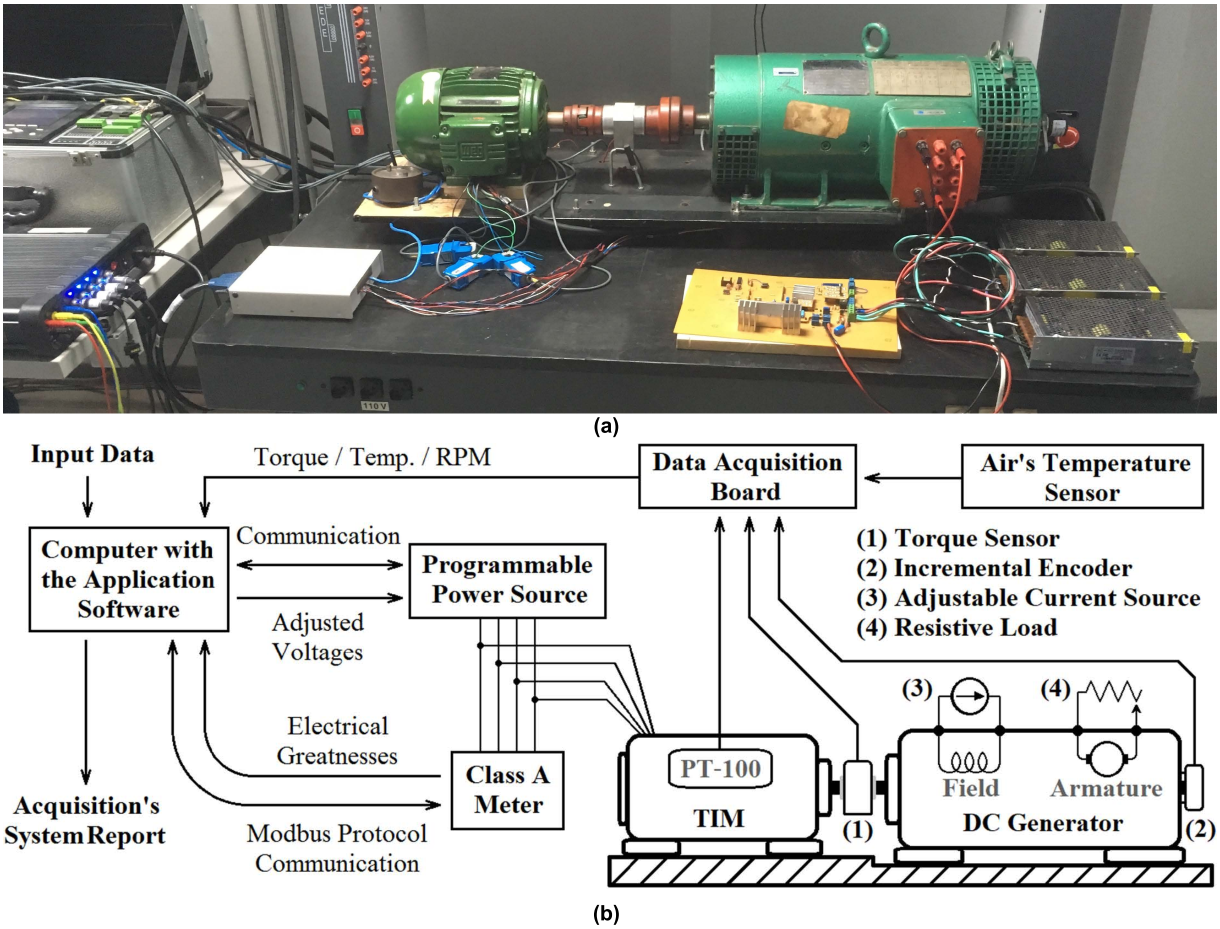

FIGURE 2. Experimental apparatus – (a) picture and (b) schematic.

V_{NOM}, which is 220V) by PRODIST [17]. Also considering that V_2 and θ_2 vary from 0% to 7.5% and from 0° to 360°, respectively, it can be concluded that the DB_1 contemplates a comprehensive set of voltage conditions found in electrical systems. In fact, the results of the application of this data bank allow, using the thermal model, to identify the temperature of the TIM for a wide-ranging set of unbalanced conditions.

The 650 conditions used in DB_2 were selected from DB_1 through a computational algorithm developed with the objective of contemplating the entire range of the sample space of electric currents (I_A, I_B and I_C) acquired with the application of the 8244 combinations of terminal voltage on the TIM.

Fig. 1 shows the values of I_A, I_B and I_C read on the stator winding of the TIM when it was applied the voltage conditions contained in databases DB_1 and DB_2.

It can be seen from Fig. 1 that DB_2 covers the entire sample space filled by the combinations of electrical currents present in DB_1. Since DB_2 lends itself to estimate the thermal parameters of TIM, this feature contributes to increasing the effectiveness of this tool.

Aiming to reduce the inaccuracies in the acquisition process of the measurements, some actions are taken during the tests. They are: the order of application of the three-phase voltages belonging to DB_1 and DB_2 are established to guarantee smooth variations between consecutive conditions; and to reach the warm up time at the beginning or in cases of test discontinuity, the TIM was submitted to its rated and balanced voltages for two and a half consecutive hours. It should be noted that the temperature resulting from this condition is considered as the nominal temperature (T_{NOM}).

B. THE LABORATORY APPARATUS

For the application of the balanced and unbalance voltages on the TIM and the automatic collection of the currents, temperatures, powers and rotational velocities, we developed a closed loop control system, shown in Fig. 2. Such apparatus is constituted of: i) the CSW 11110 programmable source; ii) the Elspec G4500 and ION 7600 electric quantity meters; iii) the NI PCI-6251 data acquisition board from National Instruments, among other equipment.

As mentioned, to apply the proposed methodology and evaluate the performance of the WVUF, we used a TIM. It was connected in delta and has the following specifications: i) class F isolation; ii) rated output power of 1.5 kW; iii) rated currents and line voltages of 6.15 A and 220 V, respectively;

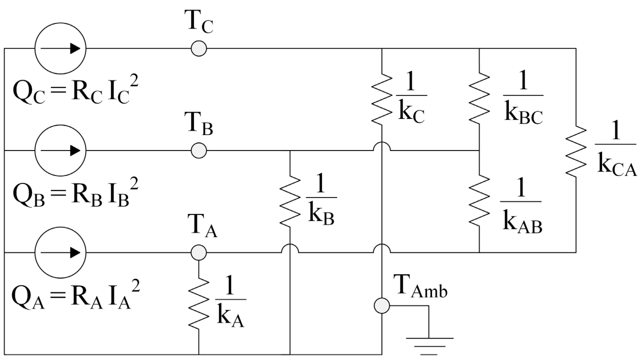

FIGURE 3. Equivalent thermal circuit for estimating the temperatures of the TIM.

TABLE 2. Parameters of the thermal model.

k_A (W/K)	k_B (W/K)	k_C (W/K)	k_{AB} (W/K)	k_{BC} (W/K)	k_{CA} (W/K)	R_A (Ω)	R_B (Ω)	R_C (Ω)
1.067	1.048	1.062	1.091	1.110	1.037	4.464	4.456	4.331

TABLE 3. Base values employed in the tests.

Quantities	Acronyms	Nominal Values
Voltage (V)	V_{NOM}	220 V
Efficiency (%)	η_{NOM}	84.2%
Temperature (°C)	T_{NOM}	79.4 °C

and iv) a PT-100 temperature sensor connected at the end winding of each phase of the stator. A 4 kW DC generator was used as a linear load with its field coil fed by a regulated current source. Its armature coil was connected to a resistive load, which was selected so that when the rated and balanced voltages feed the TIM, the nominal current is reached.

C. THERMAL MODEL OF THE INDUCTION MOTOR

The values of the temperature of the TIM were calculated using the set of measured currents of DB_1. For this, the thermal circuit shown in Fig. 3 and detailed in [22] was used to identify the steady state temperatures of the TIM under test. In this figure, the 'A', 'B', 'C' and 'Amb' indexes represent the phases in the stator windings and the physical environment external to the TIM, respectively. T_A, T_B, T_C and T_{Amb} are the temperature in degrees Celsius; I_A, I_B and I_C are the input currents in Amperes; R_A, R_B and R_C are the electric resistance in Ohms; Q_A, Q_B and Q_C are the heat produced in Watts; k_{AB}, k_{BC} and k_{CA} are the thermal conductivity between the phases in Watt per degrees Celsius; and k_A, k_B and k_C are the thermal conductivity between the phases and the physical environment external to the TIM.

The values of T_A, T_B and T_C are obtained by applying (14). This equation can be used for both balanced and unbalanced voltage conditions.

$$[T_A\ T_B\ T_C]^T = [K]^{-1} \times [R_A I_A^2\ R_B I_B^2\ R_C I_C^2]^T \quad (14)$$

where:

$$[K] = \begin{bmatrix} k_A + k_{AB} + k_{CA} & -k_{AB} & -k_{CA} \\ -k_{AB} & k_B + k_{AB} + k_{BC} & -k_{BC} \\ -k_{CA} & -k_{BC} & k_C + k_{BC} + k_{CA} \end{bmatrix} \quad (15)$$

For the calculation of R_A, R_B, R_C and the elements of the [K] matrix, we employed the least squares optimization method. This technique guarantees a high degree of accuracy in the estimation of the operating temperatures of the TIM submitted to VU, as demonstrated in [22].

The procedures for obtaining the thermal parameters are constituted of two stages. Initially, the reading of the electrical currents and temperatures of the TIM subjected to the 650 unbalanced conditions of DB_2 was carried out in laboratory. Then, the acquired electric currents and temperatures were used respectively as input and output quantities in the computational tool capable of providing the combination of the parameters that best represents the temperatures of the TIM at steady state.

Table 2 exhibits the values obtained for the parameters of the thermal model of the TIM under study. When comparing the measured temperatures resulting from the application of DB_2 on the TIM with those acquired by the thermal model, we verified that the average error between them is 1.8 °C, which corresponds to 2.5% of T_{NOM}. Therefore, it is possible to observe that the method used in this study is effective in estimating the temperatures in the windings of the TIM under test.

V. RESULTS OF THE ELABORATION OF THE WVUF

In this section, the results from the application of the methodology that culminates in the WVUF are presented. Subsequently, the results of the comparative assessment between the VUF, LVUR, PVUR and WVUF are exposed to prove the effectiveness of the index that will be obtained.

In the analysis that follows, the voltages and η are expressed as a percentage of their nominal values specified by the manufacturer. The T is described in percentage of T_{NOM}. Table 3 shows the nominal values adopted in this study.

A. MODELING THE AVERAGE BEHAVIOR OF THE TIM TEMPERATURE AND EFFICIENCY VARIATIONS

Considering the laboratorial apparatus and the thermal model detailed previously, it is possible to get the T and η from the TIM under test, according to the conditions of DB_1.

Fig. 4(a) and (b) respectively show the experimental curves of T and η in function of V_2. In an analogous way, Fig. 4(c) and (d) show the experimental curves of T and η in function of V_1. Given that DB_1 is composed of 9 different values of V_1, 16 values of V_2 and 60 of θ_2, in the graphs of Fig. 4(a) and (b), there are 540 curves resulting from the possible combinations of V_1 with θ_2. In the same way, in the graphs of Fig. 4(c) and (d), there are 901 curves resulting from

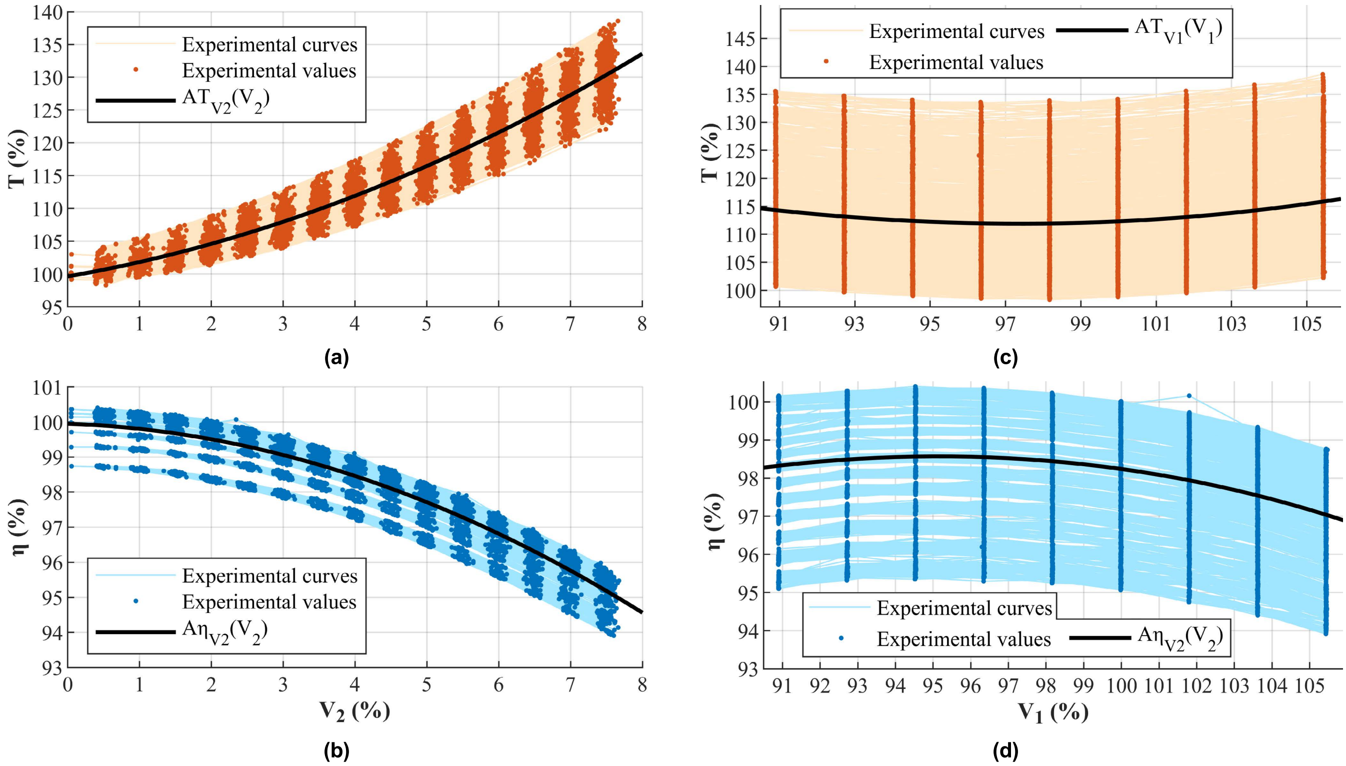

FIGURE 4. Behavior of the (a) T in function of V_2; (b) η in function of V_2; (c) T in function of V_1; and (d) η in function of V_1.

the possible combinations of V_2 with θ_2 (when $V_2 = 0\%$, θ_2 do not vary). The experimental curves in Fig. 4 were obtained by applying curve fitting method. The black curves, given by (16) and (17), are the average behavior of the T ($AT_{V2}(V_2)$) and η ($A\eta_{V2}(V_2)$) in function of V_2. Similarly, the black curves given by (18) and (19), are the average behavior of the T ($AT_{V1}(V_1)$) and η ($A\eta_{V1}(V_1)$) in function of V_1. Each coefficient of (16) and (17) corresponds to the mean of the 540 respective coefficients presented in each one of the 540 equations acquired. The expressions shown in (18) and (19) were obtained by performing the same procedure.

$$AT_{V_2}(V_2) = 0.2909V_2^2 + 1.9030V_2 + 99.63\% \quad (16)$$

$$A\eta_{V_2}(V_2) = -0.0750V_2^2 - 0.0720V_2 + 99.95\% \quad (17)$$

$$AT_{V_1}(V_1) = 5.82\times10^{-6}V_1^4 - 1.14\times10^{-3}V_1^3 + 0.0555V_1^2 + 111.96\% \quad (18)$$

$$A\eta_{V_1}(V_1) = -1.33\times10^{-6}V_1^4 + 2.53\times10^{-4}V_1^3 - 0.0120V_1^2 + 98.54\% \quad (19)$$

The variations of T and η in function of V_2 and V_1, which are $BT_{V2}(V_2)$, $B\eta_{V2}(V_2)$, $BT_{V1}(V_1)$ and $B\eta_{V1}(V_1)$, are given by:

$$BT_{V_2}(V_2) = T_{AVG(V_2)} - 99.63\% \quad (20)$$

$$B\eta_{V_2}(V_2) = 99.95\% - \eta_{AVG(V_2)} \quad (21)$$

$$BT_{V_1}(V_1) = T_{AVG(V_1)} - 111.96\% \quad (22)$$

$$B\eta_{V_1}(V_1) = 98.54\% - \eta_{AVG(V_1)} \quad (23)$$

These equations were obtained by eliminating the constant values from (16) to (19), and multiplying (17) and (19) by –1 so that the variations of η became positive, that is, in the same direction of the variations of T.

Fig. 5(a) and (b) respectively present the experimental curves of T and η in function of θ_2 and V_2 for different combinations of V_2 and V_1. In these graphs, different colors are used to depict the amplitude of V_2. Considering that DB_1 is composed of 9 different values of V_1 and 16 of V_2, in each of these graphs, there are 144 curves resulting from the possible combinations of V_1 with V_2.

On analyzing Fig. 5(a), it is verified that the influence of θ_2 on the T of the TIM is proportional to the amplitude of V_2, and has a sinusoidal behavior. Proceeding as done for V_2 and V_1, it is possible to obtain the average curves that represent the variation of T in function of V_2 and θ_2 ($BT_{\theta 2}(\theta_2, V_2)$), which is given by (24).

$$BT_{\theta_2}(\theta_2, V_2) = 1.2965V_2 \cdot \left|\sin\left(\frac{\pi}{120}\theta_2 - 0.5470\right)\right| \quad (24)$$

From Fig. 5(b), it is possible to infer that the variation of η in function of θ_2 is not significant.

B. MODELING THE JOINT WEIGHTED AVERAGE BEHAVIOR OF THE TIM TEMPERATURE AND EFFICIENCY VARIATIONS

To assign the same weight to T and η in the average model, some normalization must be carried out in the scale of the axis. The implementation of the normalization in the scale

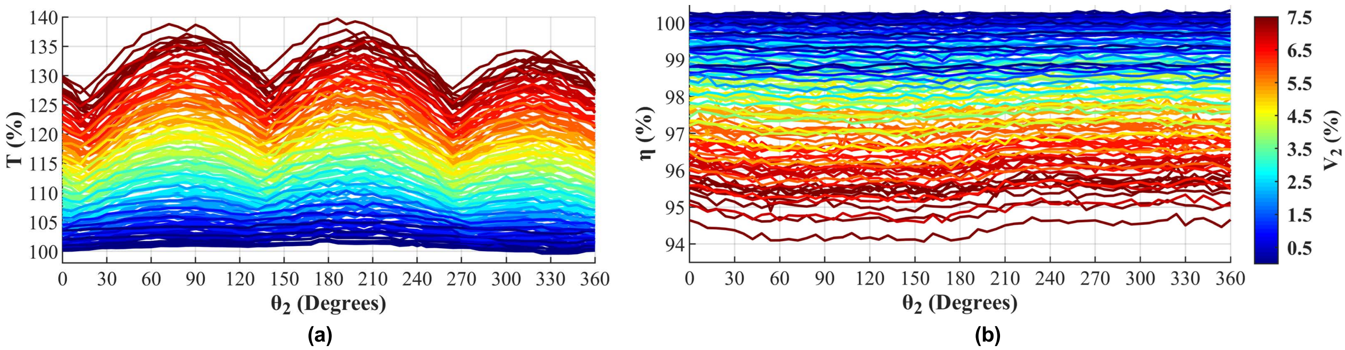

FIGURE 5. Behavior of the (a) T and (b) η of the TIM under test in function of θ_2 and V_2.

of T was performed through the multiplication of $BT_{V2}(V_2)$, $BT_{V1}(V_1)$ and $BT_{\theta 2}(\theta_2,V_2)$ by 0.217. In the case of the η, the terms $B\eta_{V2}(V_2)$ and $B\eta_{V1}(V_1)$ must be multiplied by 1.194. The value 0.217 resulted from the following procedure:

1) Initially, the highest values of $BT_{V2}(V_2)$ and $BT_{V1}(V_1)$, obtained from the measurements carried out on the TIM under test, respectively, 30.64% (for $V_2 = 7.5\%$) and 3.92% (for $V_1 = 105.5\%$), are added;

2) The result of this sum, which corresponds to 34.56%, is taken as equivalent to the 7.5%. The choice of this level (7.5%) was made so that the scale of the WVUF became similar to that of VUF. By dividing 7.5% by 30.64%, we reached the value of 0.217. Therefore, when analyzing the temperature, all values of (20), (22) and (24) should be multiplied by the 0.217 factor.

The value 1.194 is obtained by performing a procedure similar to the one used for $BT_{V2}(V_2)$ and $BT_{V1}(V_1)$. In this case, however, the sum of $B\eta_{V2}(V_2) = 4.75\%$ and $BT_{V1}(V_1) = 1.53\%$, related to $V_2 = 7.5\%$ and $V_1 = 105.5\%$, is assumed to correspond to 7.5%.

The changes in scales described above were applied in (20) to (24), resulting in $CT_{V2}(V_2)$, $C\eta_{V2}(V_2)$, $CT_{V1}(V_1)$, $C\eta_{V1}(V_1)$ and $CT_{\theta 2}(\theta_2,V_2)$, which are given by (25) to (29), respectively.

$$CT_{V_2}(V_2) = 0.0631V_2^2 + 0.4131V_2 \tag{25}$$

$$C\eta_{V_2}(V_2) = 0.0895V_2^2 + 0.0859V_2 \tag{26}$$

$$CT_{V_1}(V_1) = 1.26\times10^{-6}V_1^4 - 2.47\times10^{-4}V_1^3 + 0.0120V_1^2 \tag{27}$$

$$C\eta_{V_1}(V_1) = 1.58\times10^{-6}V_1^4 - 3.02\times10^{-4}V_1^3 + 0.0144V_1^2 \tag{28}$$

$$CT_{\theta_2}(\theta_2, V_2) = 0.2813V_2 \cdot \left|\sin\left(\frac{\pi}{120}\theta_2 - 0.547\right)\right| \tag{29}$$

The $F(V_2)$, $G(V_1)$ and $H(\theta_2,V_2)$ models that represent the weighted average behavior resulting from the joint approach of the variations of the T and η of TIM in relation to V_2, V_1 and θ_2 were obtained by applying (25) to (29) in (11) to (13).

In order to identify each combination of weight used in the WVUF, we elaborated a nomenclature, namely, $WVUF_{WF,WG,WH}$, where the sub-indexes W_F, W_G and W_H represent the weights (in percentage) adopted in (11) to (13).

C. FORMULATION OF THE WVUF

According to (10), the WVUF results from the sum of the $F(V_2)$, $G(V_1)$ and $H(\theta_2,V_2)$ models. Using, for example, $W_F = W_G = W_H = 0.5$ in (11) to (13), the $WVUF_{50,50,50}$ is given by:

$$\begin{aligned} WVUF_{50,50,50}(\%) = {} & 0.0763V_2^2 + 0.2495V_2 \\ & + 1.42\times10^{-6}V_1^4 - 2.74\times10^{-4}V_1^3 \\ & + 0.0132V_1^2 + 0.1407V_2 \\ & \cdot \left|\sin\left(\frac{\pi}{120}\theta_2 - 0.5470\right)\right| \end{aligned} \tag{30}$$

From (30), it is possible to verify that, once the weights of W_F, W_G and W_H have been established, the $WVUF_{WF,WG,WH}$ can be written in a general way as (31).

$$\begin{aligned} WVUF_{W_F,W_G,W_H}(\%) = {} & aV_2^2 + bV_2 + cV_1^4 + dV_1^3 + eV_1^2 \\ & + fV_2 \cdot \left|\sin\left(\frac{\pi}{120}\theta_2 + g\right)\right| \end{aligned} \tag{31}$$

where the coefficients 'a' to 'g' are resultant from algebraic manipulations involving the chosen W_F, W_G and W_H values and the terms from the $F(V_2)$, $G(V_1)$ and $H(\theta_2,V_2)$ models.

VI. RESULTS FROM THE VOLTAGE UNBALANCE INDEXES EVALUATION

The evaluation of the VUF, PVUR, LVUR and WVUF was performed by comparing their T and η variation ranges for each level of VU. This is a direct and effective way to assess how the mentioned indexes associate their magnitudes to the effects caused by the VU.

According to (11) to (13), the WVUF is composed by the $F(V_2)$, $G(V1)$ and $H(\theta_2,V_2)$ models, which are related to the V_2, V_1 and θ_2, in this order. The $F(V_2)$ represents the weighted average behavior resulting from the joint approach of the variations of the T and η of the TIM in function of V_2, and $G(V_1)$ and $H(\theta_2,V_2)$ are related to V_1 and θ_2, respectively. Aiming to verify the contributions of T and η for V_2, V_1 and θ_2, we stablished the weights W_F, W_G and W_H (in the range between 0% and 100%) assigned to the T in the $F(V_2)$,

TABLE 4. Coefficients of the WVUF considering the adopted weights of W_F, W_G and W_H.

	a	*b*	*c*	*d*	*e*	*f*	*g*
$WVUF_{50,50,50}$	0.07629	0.24948	1.42×10^{-6}	-2.74×10^{-4}	0.01320	0.14067	–0.54698
$WVUF_{50,50,100}$	0.07629	0.24948	1.42×10^{-6}	-2.74×10^{-4}	0.01320	0.28134	–0.54698
$WVUF_{50,50,0}$	0.07629	0.24948	1.42×10^{-6}	-2.74×10^{-4}	0.01320	0	0
$WVUF_{100,100,100}$	0.06313	0.41305	1.26×10^{-6}	-2.47×10^{-4}	0.01204	0.28134	–0.54698
$WVUF_{0,0,0}$	0.08946	0.08592	1.58×10^{-6}	-3.02×10^{-4}	0.01437	0	0

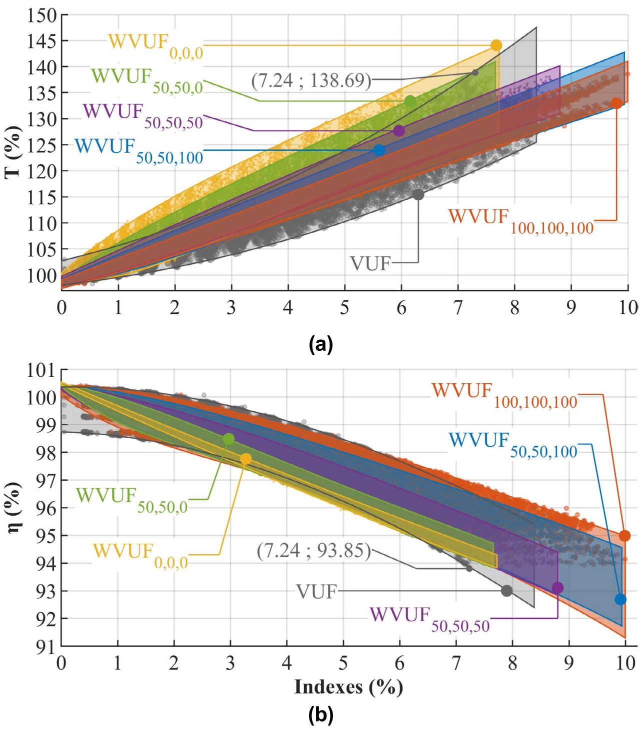

FIGURE 6. Values and envelops of (a) T and (b) η of TIM in function of the indexes VUF, $WVUF_{50,50,50}$, $WVUF_{50,50,100}$, $WVUF_{50,50,0}$, $WVUF_{100,100,100}$ and $WVUF_{0,0,0}$.

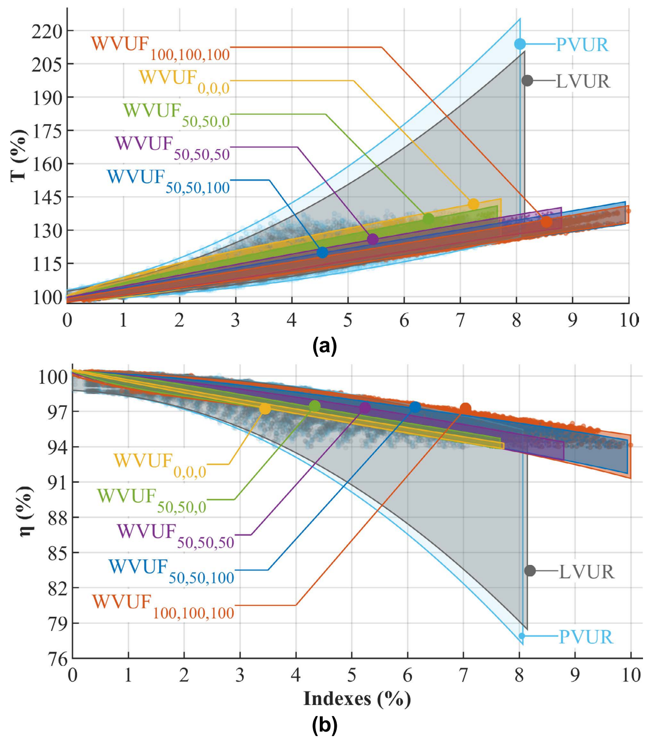

FIGURE 7. Values and envelops of (a) T and (b) η of TIM in function of the indexes LVUR, PVUR, $WVUF_{50,50,50}$, $WVUF_{50,50,100}$, $WVUF_{50,50,0}$, $WVUF_{100,100,100}$ and $WVUF_{0,0,0}$.

$G(V_1)$ and $H(\theta_2,V_2)$ functions. Strategically, in this study we opted to evaluate the results from the conditions of weights that were: i) $WVUF_{100,100,100}$ with the contributions of only T in the $F(V_2)$, $G(V_1)$ and $H(\theta_2,V_2)$ models; ii) $WVUF_{0,0,0}$ with the contributions of only η in the $F(V_2)$, $G(V_1)$ and $H(\theta_2,V_2)$ models; iii) $WVUF_{50,50,50}$ with the same contributions of T and η in the $F(V_2)$, $G(V_1)$ and $H(\theta_2,V_2)$ models; iv) $WVUF_{50,50,0}$ with the same contributions of T and η in the $F(V_2)$, $G(V_1)$ models. In this case, we do not have contributions of T in $H(\theta_2,V_2)$; and v) $WVUF_{50,50,100}$ with the same contributions of T and η in the $F(V_2)$, $G(V_1)$ models. In this case, we have only contributions of T in $H(\theta_2,V_2)$.

It should be highlighted that, with the choice of the five abovementioned conditions, we contemplated all the ranges of the contributions from T and η in the $F(V_2)$, $G(V_1)$ and $H(\theta_2,V_2)$ models. These are the reasons for the selection of these five sets of weights.

Table 4 shows the coefficients '*a*' to '*g*' of (31) according to the $WVUF_{50,50,50}$, $WVUF_{50,50,100}$, $WVUF_{50,50,0}$, $WVUF_{100,100,100}$ and $WVUF_{0,0,0}$.

Fig. 6(a) and (b) respectively show the experimental measured values (dots) of T and η and their envelopes as a function of the VUF, $WVUF_{50,50,50}$, $WVUF_{50,50,100}$, $WVUF_{50,50,0}$, $WVUF_{100,100,100}$ and $WVUF_{0,0,0}$, when DB_1 was applied.

In an analogous way, Fig. 7(a) and (b) respectively show the experimental measured values (dots) of T and η and their envelopes as a function of LVUR, PVUR, $WVUF_{50,50,50}$, $WVUF_{50,50,100}$, $WVUF_{50,50,0}$, $WVUF_{100,100,100}$ and $WVUF_{0,0,0}$.

It may be observed from graphs of Figs. 6 and 7 that, although the set of balanced and unbalanced voltages of DB_1 applied to the TIM was the same, the maximum values of VUF, PVUR, LVUR, $WVUF_{50,50,50}$, $WVUF_{50,50,100}$, $WVUF_{50,50,0}$, $WVUF_{100,100,100}$ and $WVUF_{0,0,0}$ are different.

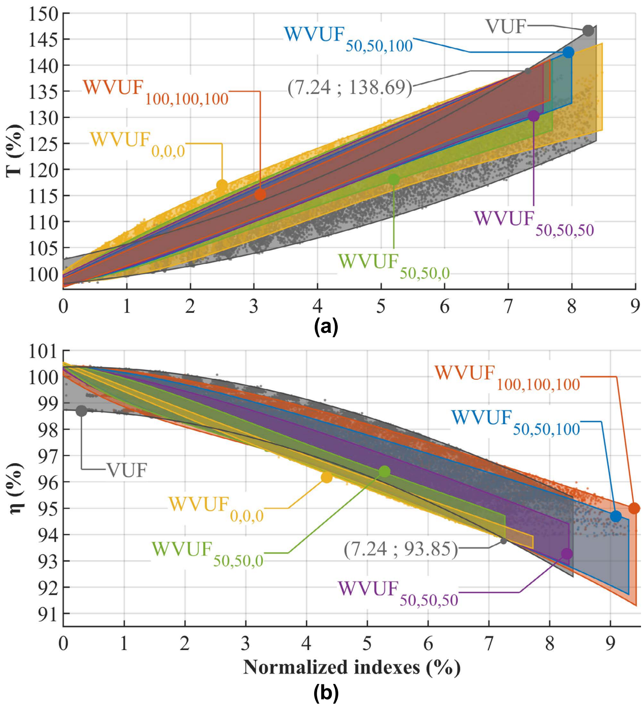

FIGURE 8. The variation regions of (a) the T and (b) the η for VUF, $WVUF_{50,50,50}$, $WVUF_{50,50,100}$, $WVUF_{50,50,0}$, $WVUF_{100,100,100}$ and $WVUF_{0,0,0}$ indexes.

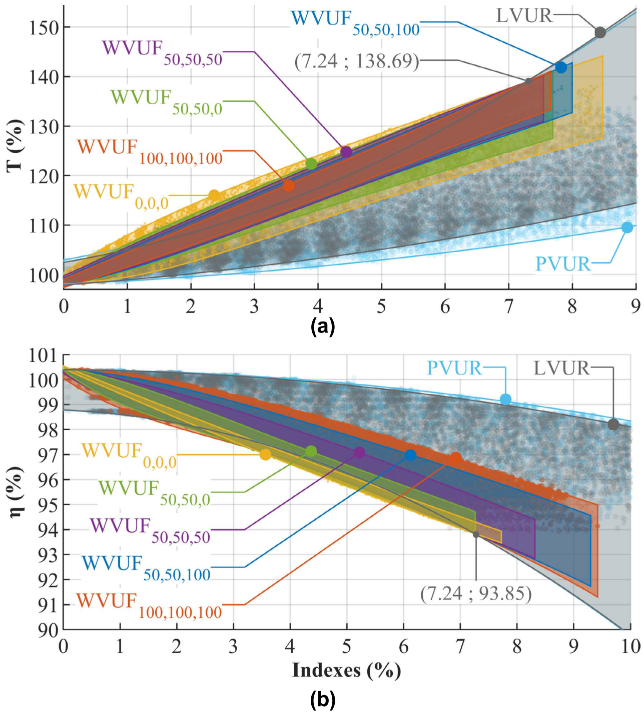

FIGURE 9. The variation regions of (a) the T and (b) the η for, LVUR, PVUR, $WVUF_{50,50,50}$, $WVUF_{50,50,100}$, $WVUF_{50,50,0}$, $WVUF_{100,100,100}$ and $WVUF_{0,0,0}$ indexes.

This occurred because these indexes have their own scales. Therefore, aiming to comparatively evaluate the mentioned indexes, some changes in scale of the WVUF must be performed. It is important to emphasize that such adjustments do not properly modify the formulations of the indexes. To do so, the following procedure was adopted:

1) Initially, one index should be chosen as the reference. In this work, we opted to use the VUF.

2) We identify the maximum value of T from the laboratory tests and the VUF related to this measurement. They are T = 138.69% for VUF = 7.24%.

3) Then, T = 138.69% is associated with the conditions in which the PVUR, LVUR, $WVUF_{50,50,50}$, $WVUF_{50,50,100}$, $WVUF_{50,50,0}$, $WVUF_{100,100,100}$ and $WVUF_{0,0,0}$ are equal to 7.24%. To exemplify the effect of this change, consider the case of PVUR. Without the change in scale, the PVUR corresponding to T = 138.69% is equal to 3.75%. With the proposed change, the PVUR is equal to 7.24% for the condition in which T = 138.69%. Consequently, when analyzing the T, all values of PVUR should be multiplied by the factor 7.24/3.75 = 1.93.

Regarding the η, we identified 93.85% (for VUF = 7.24%) as the minimum value measured in the laboratory tests and associated it with the conditions in which the PVUR, LVUR, $WVUF_{50,50,50}$, $WVUF_{50,50,100}$, $WVUF_{50,50,0}$, $WVUF_{100,100,100}$ and $WVUF_{0,0,0}$ indexes are equal to 7.24%. In this case, by applying the same procedure adopted for T, the multiplier factor of PVUR related to η is equal to 1.95.

TABLE 5. Scale factors applied to T and η for LVUR, PVUR, $WVUF_{50,50,50}$, $WVUF_{50,50,100}$, $WVUF_{50,50,0}$, $WVUF_{100,100,100}$ and $WVUF_{0,0,0}$

Index	T	η
LVUR	1.73150	1.88220
PVUR	1.92830	1.95290
$WVUF_{50,50,50}$	0.85782	0.94517
$WVUF_{50,50,100}$	0.80479	0.93576
$WVUF_{50,50,0}$	1.00450	0.94845
$WVUF_{100,100,100}$	0.76589	0.94252
$WVUF_{0,0,0}$	1.09760	0.94128

Table 5 presents the multiplication factors employed when analyzing T and η for LVUR PVUR, $WVUF_{50,50,50}$, $WVUF_{50,50,100}$, $WVUF_{50,50,0}$, $WVUF_{100,100,100}$ and $WVUF_{0,0,0}$.

Fig. 8(a) and (b) shows the variation regions of the T and η in function of the VUF, $WVUF_{50,50,50}$, $WVUF_{50,50,100}$, $WVUF_{50,50,0}$, $WVUF_{100,100,100}$ and $WVUF_{0,0,0}$, considering the application of the changes in the scales presented in Table 5.

In the same way, Fig. 9(a) and (b) shows the variation regions of the T and η in function of the LVUR, PVUR, $WVUF_{50,50,50}$, $WVUF_{50,50,100}$, $WVUF_{50,50,0}$, $WVUF_{100,100,100}$ and $WVUF_{0,0,0}$.

To numerically evaluate the performance of the indexes presented in Figs. 8 and 9, we calculated the differences between the upper and lower limits of T and η for each VU level. With these results, we assembled Figs. 10 and 11, which respectively show the variation ranges of the correspondent

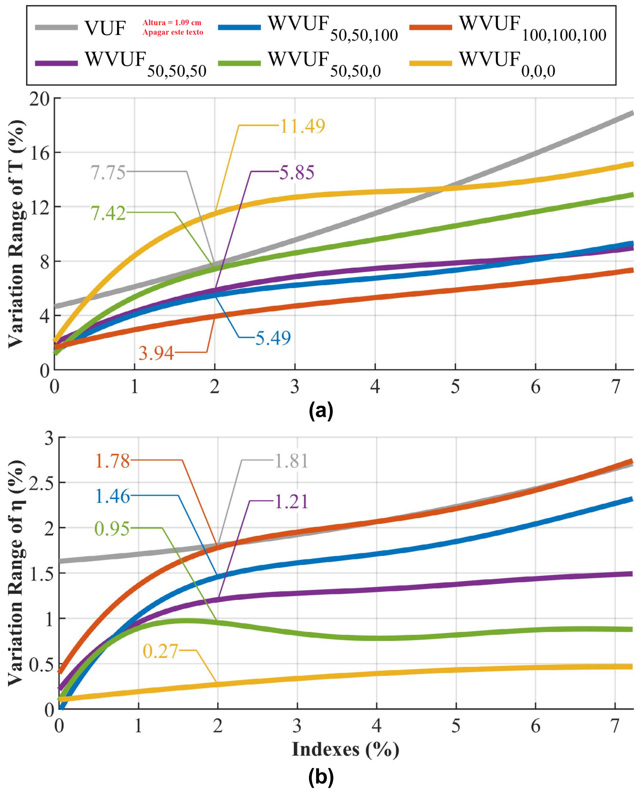

FIGURE 10. Variation ranges of (a) T and (b) η of the VUF, $WVUF_{50,50,50}$, $WVUF_{50,50,100}$, $WVUF_{50,50,0}$, $WVUF_{100,100,100}$ and $WVUF_{0,0,0}$ indexes.

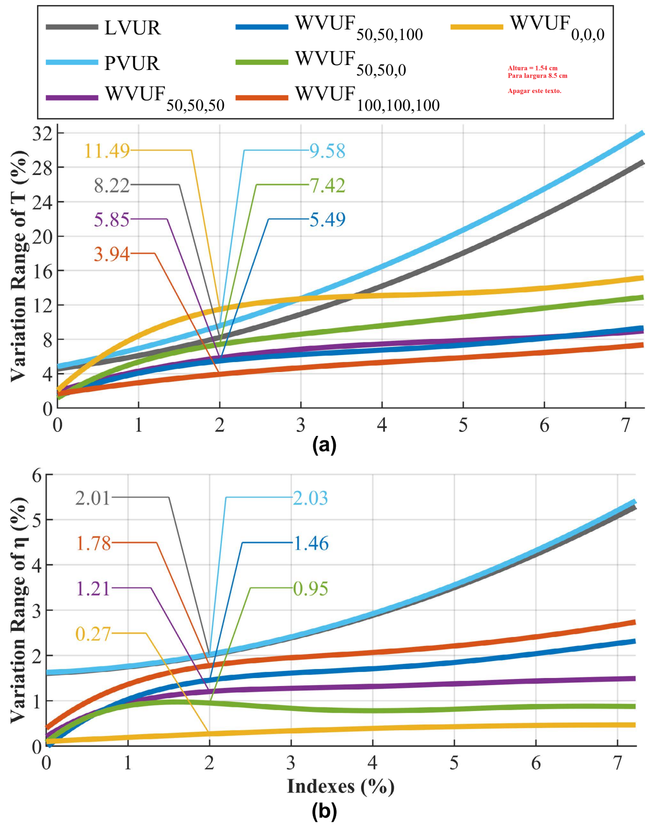

FIGURE 11. Variation ranges of (a) T and (b) η of the LVUR, PVUR, $WVUF_{50,50,50}$, $WVUF_{50,50,100}$, $WVUF_{50,50,0}$, $WVUF_{100,100,100}$ and $WVUF_{0,0,0}$ indexes.

indexes exhibited in Figs. 8 and 9. It is assumed that the lower the variation range of T or η for a given VU level, the more assertive is the index regarding its association with the effects of this phenomenon.

From Figs. 10 and 11 we can verify that for the level of VU equal to 2% (limit established for the VUF in some standards that deal with this phenomenon), the variation ranges of T when utilizing the VUF, LVUR and PVUR are respectively equal to 7.75%, 8.22% and 9.58%. In the same order, these variations are 1.81%, 2.01% and 2.03%, with respect to the η. Among the traditional indexes employed to quantify VU, the VUF presented the best performance to measure the effects of both T and η for all values of VU applied to the TIM. For this reason, the VUF was used to execute the comparative assessment with the WVUF calculated with the different weights.

It is possible to observe in Fig. 10(a) that, when the VU is equal to 2%, the variation range of T is equal to 3.94% for the $WVUF_{100,100,100}$ and 7.75% for the VUF. Therefore, the use of the $WVUF_{100,100,100}$ reduces the variation range of T by 50.8% in relation to the value obtained for the VUF. All the indexes under evaluation, except for $WVUF_{0,0,0}$, resulted in reductions of the variation ranges of T in relation to the VUF, LVUR and PVUR. Only $WVUF_{0,0,0}$ exhibited variation ranges greater than those of the VUF for the interval between 0.5% and 4.9%. The weights adopted for this index prioritize the η.

In Fig 10(b), for the level of VU equal to 2%, the variation range of η for $WVUF_{0,0,0}$ was equal to 0.27% and for the VUF was 1.81%, which means a reduction of 85% in relation to the value acquired for the VUF.

Based on the results from Figs. 10 and 11, it is possible to verify that the $WVUF_{100,100,100}$ and $WVUF_{0,0,0}$ present the best performances when individually evaluating the T and η, respectively.

Considering the indexes that jointly contemplate T and η, for the level of VU equal to 2%, the $WVUF_{50,50,50}$, $WVUF_{50,50,100}$ and $WVUF_{50,50,0}$ exhibit variation ranges for T of 24.5%, 29.2%, and 4.3% lower than those of the VUF, respectively. We can verify for this level of VU that, although the $WVUF_{50,50,100}$ has the best performance for the analysis of T, the $WVUF_{50,50,50}$ presents a significant reduction in the variation range. These aspects can be observed for most levels of VU exhibited in Figs. 10 and 11.

When evaluating the η, the variation ranges of the $WVUF_{50,50,50}$, $WVUF_{50,50,100}$ and $WVUF_{50,50,0}$ indexes are respectively 33.1%, 19.3% and 47.5% lower than those of the VUF. In this case, the $WVUF_{50,50,0}$ culminated in the best performance. Once again, the use of the $WVUF_{50,50,50}$ presented an expressive reduction in the variation ranges. This can also be verified for other levels of VU.

Given that for both T and η the use of the $WVUF_{50,50,50}$ resulted in significant reductions in the variation ranges, we assumed that it is the most appropriate weight to be used in the index for quantifying the effects of VU.

VII. CONCLUSION AND FINAL REMARKS

This work presented an alternative methodology for the quantification of VU based on the effects of this phenomenon on the temperature and η of TIM. The proposed methodology results in the WVUF index, which contemplates the nonlinear response of the temperature and η of TIM in relation to the variations of $\overline{V}_2$ and $\overline{V}_1$.

To apply this methodology and to evaluate the performance of the obtained index, we carried out some tests employing a robust laboratory apparatus developed to control several VU conditions applied on a TIM. These tests made it possible to obtain the parameters of the thermal model used in this study, as well as the T and η of the evaluated motor.

To provide information on the proposed methodology, we exhibited a detailed presentation of each step. Initially, we modeled the average behavior of the variations of the T and η of a TIM. We then obtained the models that represent the average behavior resulting from the joint weighted approach of the variations of the T and η of the TIM in function of V_2, V_1 and θ_2. Once in possession of these models, it was possible to obtain the equation of the WVUF.

The evaluation of the performance of the WVUF with different combinations of weights was done by comparing its results with those of the VUF, LVUR and PVUR. As expected, the $WVUF_{100,100,100}$ and $WVUF_{0,0,0}$ respectively showed the best performances when evaluating the T and η individually. This happened because the weights employed in the $WVUF_{100,100,100}$ prioritize the effects of T, and those utilized in the $WVUF_{0,0,0}$ focus on the η.

When dealing with the case in which the combinations of T and η are simultaneously evaluated, we identified that the combination of weights from the $WVUF_{50,50,50}$ was the most appropriate for quantifying the effects of VU. This index corresponds to that in which the T and η are weighted in the same proportion for V_1, V_2 and θ_2. It should also be mentioned that the results of T and η originating from the application of a comprehensive balanced and unbalanced voltage data bank on the TIM under test demonstrated that the $WVUF_{50,50,50}$, when compared to the VUF, significantly reduces the uncertainties inherent to the quantification process of this phenomenon. Given that the WVUF decreases the variation ranges of T and η for each level of VU, it allows a better association between the values and effects of VU.

Considering the aforementioned results, it is possible to infer that the proposed methodology resulted in an index that was able to jointly represent the effects of $\overline{V}_2$ and $\overline{V}_1$ on the T and η of motors connected to the electric system. The advantages associated with the WVUF designate it as a potential alternative to be employed in industrial utilities and standards that deal with the subject.

We are aware that the WVUF found in this study is related to the characteristics of the TIM utilized in the tests, and that there are still some challenges and demands that would need to be addressed in further research. They are the use of different electrical equipment, the consideration of the $\overline{V}_0$ in the process, and the use of TIM with different constructive aspects, manufacturers, power ratings, and load conditions. Since the proposed methodology employs the normalized curves of the T and η to obtain the WVUF, the results that will be acquired using different types of TIM are probably not significantly discrepant from those shown in this work.

REFERENCES

[1] W. E. Vanco, F. B. Silva, and J. R. B. A. Monteiro, "A study of the impacts caused by unbalanced voltage (2%) in isolated synchronous generators," *IEEE Access*, vol. 7, pp. 72956–72963, 2019.

[2] J. M. Tabora, M. E. De Lima Tostes, U. H. Bezerra, E. O. De Matos, C. L. P. Filho, T. M. Soares, and C. E. M. Rodrigues, "Assessing energy efficiency and power quality impacts due to high-efficiency motors operating under nonideal energy supply," *IEEE Access*, vol. 9, pp. 121871–121882, 2021.

[3] V. P. Brasil, J. Y. Ishihara, and A. L. F. Filho, "Fair power factor billing under unbalanced and nonsinusoidal voltage supply," *IEEE Access*, vol. 10, pp. 19301–19311, 2022.

[4] C.-Y. Lee, "Effects of unbalanced voltage on the operation performance of a three-phase induction motor," *IEEE Trans. Energy Convers.*, vol. 14, no. 2, pp. 202–208, Jun. 1999.

[5] Y.-J. Wang, "Analysis of effects of three-phase voltage unbalance on induction motors with emphasis on the angle of the complex voltage unbalance factor," *IEEE Trans. Energy Convers.*, vol. 16, no. 3, pp. 270–275, Sep. 2001.

[6] J. Faiz, H. Ebrahimpour, and P. Pillay, "Influence of unbalanced voltage on the steady-state performance of a three-phase squirrel-cage induction motor," *IEEE Trans. Energy Convers.*, vol. 19, no. 4, pp. 657–662, Dec. 2004.

[7] E. El-Kharashi, M. El-Dessouki, J. G. Massoud, A. W. Farid, and M. A. Al-Ahmar, "The use of the current complex factor to determine the precise output energy of the induction motor," *Electr. Power Syst. Res.*, vol. 154, pp. 23–36, Jan. 2018.

[8] P. Sudasinghe, U. Jayatunga, P. Commins, J. Moscrop, and S. Perera, "Dependancy of three phase induction motor derating aspects on complex voltage unbalance factor: A calorimetric and finite element simulation study," *IEEE Access*, vol. 9, pp. 147063–147071, 2021.

[9] J. L. Gonzalez-Cordoba, R. A. Osornio-Rios, D. Granados-Lieberman, R. D. J. Romero-Troncoso, and M. Valtierra-Rodriguez, "Correlation model between voltage unbalance and mechanical overload based on thermal effect at the induction motor stator," *IEEE Trans. Energy Convers.*, vol. 32, no. 4, pp. 1602–1610, Dec. 2017.

[10] M. S. Kurt, M. E. Balci, and S. H. E. A. Aleem, "Algorithm for estimating derating of induction motors supplied with under/over unbalanced voltages using response surface methodology," *J. Eng.*, vol. 1, no. 12, pp. 627–633, 2017.

[11] J. C. De Oliveira and L. M. Neto, "Induction motors thermal behaviour and life expectancy under non-ideal supply conditions," in *Proc. 9th Int. Conf. Harmon. Quality Power*, vol. 3, Oct. 2000, pp. 899–904.

[12] J. M. Corres, J. Bravo, F. J. Arregui, and I. R. Matias, "Unbalance and harmonics detection in induction motors using an optical fiber sensor," *IEEE Sensors J.*, vol. 6, no. 3, pp. 605–612, Jun. 2006.

[13] Y. P. Abbi and S. Jain, *Handbook on Energy Audit and Environment Management*. New Delhi, India: TERI Press, 2006.

[14] *IEEE 1159-2009—IEEE Recommended Practice for Monitoring Electric Power Quality*, IEEE Standard 1159-2009, Institute of Electrical and Electronics Engineers, 2009.

[15] *IEC 61000-4-30 Electromagnetic Compatibility (EMC)—Part 4-30: Testing and Measurement Techniques—Power Quality Measurement Methods*, IEC Standard 61000-4-30, International Electrotechnical Commission, 2015.

[16] *Electricity Supply—Quality of Supply. Part 2: Voltage Characteristics, Compatibility Levels, Limits and Assessment Methods*, Standard NRS 048-2:2003, Standards South Africa, 2013.

[17] *Procedimentos de Distribuiçáo de Energia Elétrica no Sistema Elétrico Nacional—PRODIST—Modulo 8 Qualidade da Energia elétrica*, PRODIST—Módulo, Agência Nacional de Energia Elétrica—ANEEL, Brasília, Brazil, 2019.

[18] H. J. B. Math and Y. H. G. Irene, *Signal Processing of Power Quality Disturbances* (Series on Power Engineering). Piscataway, NJ, USA: IEEE Press, 2006.

[19] P. Pillay and P. Hofmann, ''Derating of induction motors operating with a combination of unbalanced voltages and over- or undervoltages,'' in *Proc. IEEE Power Eng. Soc. Winter Meeting Conf.*, vol. 3, Mar. 2001, pp. 1365–1371.

[20] *Motors and Generators*, Standard MG1-1993, ANSI/NEMA, 1993.

[21] *IEEE Recommended Practice for Electric Power Distribution for Industrial Plants*, IEEE Standard 141-1993, Apr. 1994, pp. 1–768, doi: 10.1109/IEEESTD.1994.121642.

[22] M. D. de Castro e Silva, A. de Leles Ferreira Filho, G. Z. Rosa, and C. C. Abada, ''Evaluation of the performance of a simplified thermal model of a three phase induction motor submitted to voltage imbalances,'' in *Proc. 18th Int. Conf. Harmon. Quality Power (ICHQP)*, May 2018, pp. 1–6.

MARCOS D. C. SILVA received the B.E., M.Sc., and Ph.D. degrees in electrical engineering from the University of Brasília, Brasília, Brazil, in 2010, 2014, and 2020, respectively. He is currently working at Brazilian Army. His research interest includes power systems, with emphasis on power quality.

ANÉSIO DE L. FERREIRA FILHO received the Ph.D. degree in electrical engineering from the University of Brasília, Brasília, Brazil, in 2008. He is currently a Professor at the University of Brasília. His research interests include distribution systems, distributed generation, and power quality.